Gravito-Inertial Ambiguity Resolved through Head Stabilisation

Ildar Farkhatdinov, Hannah Michalska, Alain Berthoz, Vincent Hayward

PROCEEDINGS A

rspa.royalsocietypublishing.org

Research

Article submitted to journal

Subject Areas:
computational biology, biomedical engineering

Keywords:
head stabilisation, vestibular system, verticality, nonlinear observability, feedback

Author for correspondence:
Ildar Farkhatdinov
e-mail: i.farkhatdinov@qmul.ac.uk

Gravito-Inertial Ambiguity Resolved through Head Stabilisation

Ildar Farkhatdinov[1,2], Hannah Michalska[3] Alain Berthoz[4] and Vincent Hayward[5]

[1]School of Electronic Engineering and Computer Science, Queen Mary University of London, Mile End, London, UK
[2]Department of Bioengineering, Imperial College of Science, Technology and Medicine, South Kensington, London, UK
[3]Department of Electrical and Computer Engineering, McGill University, Montréal, Qc, Canada
[4]Centre Interdisciplinaire de Biologie (CIRB). Collége de France, 11 place Marcelin Berthelot, 75005 Paris, France
[5]Sorbonne Universités, Institut des Systèmes Intelligents et de Robotique (ISIR), F-75005, Paris, France

It has been frequently observed that humans and animals spontaneously stabilise their heads with respect to the gravitational vertical during body movements even in the absence of vision. The interpretations of this intriguing behaviour have so far not included the need, for survival, to robustly estimate verticality. Here we use a mechanistic model of the head/otolith-organ to analyse the possibility for this system to render verticality 'observable', a fundamental prerequisite to the determination of the angular position and acceleration of the head from idiothetic, inertial measurements. The intrinsically nonlinear head-vestibular dynamics is shown to generally lack observability unless the head is stabilised in orientation by feedback. Thus, our study supports the hypothesis that a central function of the physiologically costly head stabilisation strategy is to enable an organism to estimate the gravitational vertical and head acceleration during locomotion. Moreover, our result exhibits a rare peculiarity of certain nonlinear systems to fortuitously alter their observability properties when feedback is applied.

THE ROYAL SOCIETY PUBLISHING

1. Introduction

One of the main functions of the vestibular system is to provide humans and animals with sensory inputs needed to achieve and maintain balance. This function is particularly important during locomotion since, regardless of the number of limbs in contact with the ground, dynamic balance is obtained by actively counteracting both inertial and gravitational forces with reaction forces on the ground. Dynamic balance would be impossible to achieve without the knowledge of the direction of gravity in earth-related coordinates. Even quasi-statically, stable postures require one to align the centre of mass of the body and limbs directly above the region of contact with the ground.

The vestibular system comprises two types of organs. The semicircular canals respond primarily to angular velocity while the otolith organs sense translational acceleration. In each ear, the otolith organ comprises two liquid-filled chambers, where the relative displacement of otolith masses are picked up by populations of hair cells. These chambers, the utricle and the saccule, are geometrically arranged to be sensitive to certain translational acceleration components and to tilt. When the head is upright (the head's longitudinal axis is aligned with the gravitational vertical), the saccule is vertical and responds to acceleration in the sagittal plane, i.e., forward-backward and up-and-down movements. The utricle is horizontally oriented and responds to accelerations in the transverse plane [1].

Ordinary vector addition dictates that any measurement of acceleration must combine the signal due to the translational acceleration of the sensor with a signal due to the ambient gravitational component. On earth during typical movements, these components are difficult to disentangle. For that reason, a sensory ambiguity arises between tilt and translational acceleration [2,3], which can give rise to 'somatogravic' illusions (erroneous estimation of 'up' and 'down') [4], spatial disorientation, and loss of postural balance. Thus, it is only when the head is still that the otolith organs of the vestibular system provide us with a sense of absolute verticality [5,6].

The vestibular system participates in a number of important functions such as the establishment of the vestibulo-ocular and the vestibulo-collic reflexes which are respectively responsible for stabilising the gaze and the head in space, [7–9]. These reflexes are therefore closely related to the results of our study.

Head stabilisation in the upright position independent of movements of the body and the limbs is one behaviour that is widely reported in the neuroscience literature. The head stabilisation strategy has been observed in numerous species, including most of the fast moving mammals and birds, and during the execution of multiple tasks [6,10–33]. The apparent universality of this strategy, which requires a complicated articulated neck and sensorimotor control, is a testimony to its probable importance as an evolutionary advantage.

We envision the following hypotheses: a head stabilisation strategy enables an organism to simultaneously estimate the gravitational vertical and the head acceleration (H_1); and head upright stabilisation during locomotion results in the possible application of a linearised system model that facilitates gravito-inertial ambiguity resolution (H_2). To test these hypotheses, we investigated the head stabilisation strategy using the tools of systems and control theory.

The notion of observability is a central concept in this theory. Observability describes in a formal manner which quantities, be they states or unknown inputs, can be determined from the measurements made from a given system. A quantity that is not observable cannot be estimated. In the case of finite dimensional linear systems, or systems that can be assimilated as such, this question was settled fifty years ago by R. E. Kalman [34]. For nonlinear systems, of which articulated mechanical systems form an important class, the determination of observability requires the use of difficult Lie-algebraic techniques. Practical results are surprisingly sparse and so far apply only to systems of trivial complexity.

In the foregoing, we recall the development of a mechanistic model of the head and the otolith organs and justify the ability of this model to capture the fundamental dynamic properties of

the biological organ in three dimensions. The model then enabled us to express the dynamics of the head/otolith-organ structure in a mathematical form suitable for its analysis as a *bona fide* system with inputs, outputs, and states. Having gained the ability to model the head/otolith-organ system in algebraic terms, which treats the torque applied to the head and its acceleration as unknown inputs, we applied a computer-based probabilistic tool to determine if and when the direction of the vertical, together with acceleration of the head, is observable in absolute world coordinates. Our results can be summarised as follows:

(i) If the head is allowed to move freely, our analysis shows (with high probability) that head orientation and acceleration both fail to be observable;
(ii) Observability is achieved if the head is feedback controlled to a fixed orientation with no other external reference but the ambient gravity field;
(iii) This result exhibits a rarely encountered peculiarity of nonlinear systems where observability properties can be modified by the application of feedback. Such a property is not shared by linear systems;
(iv) A by-product of the feedback stabilisation of the head is to linearise an inherently nonlinear system, enabling the application of simple observer and controller designs in the planar case;
(v) Observability, as restored by the application of feedback, makes it possible to resolve the ambiguity between tilt and acceleration.

These results support strongly the hypotheses H_1 and H_2, and our findings suggest that the quasi-universally observed head stabilisation reflex has evolved as a result of the crucial advantage that it provides by making the estimation of the gravitational vertical possible during movement. The significance of our finding is not limited to the biological phenomenon considered, but is directly relevant to the general problem of verticality estimation from non-inertial platforms during spatial motion.

In the rest of this article, the methods used in the observability and identifiability analysis are first described by deriving the mathematical equations governing the dynamics of a mechanistic model of the otolith organ tucked inside the inner ear. The algebraic observability and identifiability properties of a system are then recalled and their analysis applied to the full dynamics of the otolith-head model, with and without feedback. The closed loop system can then be linearised to enable the application of the separation principle from which an observer and a controller are designed. Even in the case of a simplified linearised system around an operating point, the tilt/acceleration ambiguity resolution could be demonstrated for locomotion in the planar case with head orientation stabilisation in the sagittal plane.

2. Methods and Result

The otolith organ of the vestibular system is mechanical in nature, it is therefore reasonable to derive its properties from the laws of multi-body dynamics in three dimensions.

(a) Mechanistic Model of the Otolith Organ

The head is modelled as a rigid body displacing and orienting with six degrees of freedom in space. The head, subjected to external forces, moves relative to an inertial frame, $\mathbb{I}$, comprising the unit vectors, $\left\{{}^{\mathbb{I}}\boldsymbol{i}, {}^{\mathbb{I}}\boldsymbol{j}, {}^{\mathbb{I}}\boldsymbol{k}\right\}$, as depicted in Fig. 1. A non-inertial, body-fixed frame, $\mathbb{H} = \left\{{}^{\mathbb{H}}\boldsymbol{i}, {}^{\mathbb{H}}\boldsymbol{j}, {}^{\mathbb{H}}\boldsymbol{k}\right\}$, is assigned to the head with the origin coinciding with the center of mass. The usual anatomical division of the head by the coronal, sagittal, and transverse planes coincide with the subspaces span$\{{}^{\mathbb{H}}\boldsymbol{i}, {}^{\mathbb{H}}\boldsymbol{k}\}$, span$\{{}^{\mathbb{H}}\boldsymbol{j}, {}^{\mathbb{H}}\boldsymbol{k}\}$, span$\{{}^{\mathbb{H}}\boldsymbol{j}, {}^{\mathbb{H}}\boldsymbol{i}\}$, respectively.

Any motion of the head that leaves the vector ${}^{\mathbb{H}}\boldsymbol{k}$ invariant in the inertial frame will be referred to as motion in the transverse plane. The angle of rotation about ${}^{\mathbb{H}}\boldsymbol{k}$ is called the yaw angle and

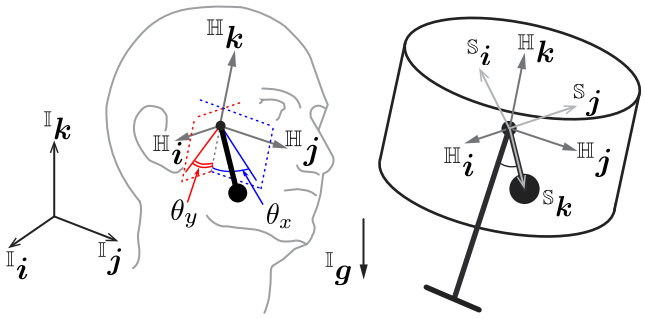

Figure 1. Coordinates assignment.

will be zero when the nose points in the direction of ${}^{\mathbb{I}}\boldsymbol{j}$. Similarly, motions that leaves the vector ${}^{\mathbb{H}}\boldsymbol{i}$ or the vector ${}^{\mathbb{H}}\boldsymbol{j}$ invariant in the inertial frame will be referred to as motion in the sagittal plane or in the coronal plane, respectively.

The head is said to be fully stabilised when all the axes of $\mathbb{H}$ are aligned with those of $\mathbb{I}$. This condition is normally achieved asymptotically only. Partial stabilisation can also be considered; e.g. when one of the three anatomical planes coincides with one plane of the inertial frame. The otolith organ is modelled as a spherical pendulum with three additional degrees of freedom constrained by a pivot at the center of mass of the head, again see Fig. 1. The otolith organ is mechanical in nature and its behaviour can be described with the mechanical pendulum model responding to gravity and acceleration as justified in the next subsection. The pendulum is damped so that its motions die out when the head is stationary. The body-fixed moving reference frame, $\mathbb{S} = \left\{{}^{\mathbb{S}}\boldsymbol{i}, {}^{\mathbb{S}}\boldsymbol{j}, {}^{\mathbb{S}}\boldsymbol{k}\right\}$, is assigned to the pendulum. The origin of this frame is located at the pivot with ${}^{\mathbb{S}}\boldsymbol{k}$ aligned with the arm of the pendulum.

The resulting model forms a dynamical system with nine degrees of freedom moving in the gravitational field, ${}^{\mathbb{I}}\boldsymbol{g}$, under the additional influence of external forces capable of translating and rotating the head.

(b) Justification of the Mechanistic Model

To justify the relevance of a seemingly oversimplified model of the organ under study, it is necessary to recall the anatomy and the function of the vestibular organs.

Later, we will see that the absolute orientation of the head is generally not an observable quantity. If the semicircular canals do provide information about the head angular velocity, such information is of no help to transform head orientation into an observable quantity. Angular velocity information can contribute to improving the estimation of the absolute head orientation only if it can be made observable.

On the other hand, the very origin of the sensation of gravitational and translational acceleration of the head is owed to the movements of the calcium carbonate bodies called otoliths which are located in the saccule and the utricle. The otoliths move relative to the inner surface of these cavities—termed the macula—under the action of gravity and of the so-called 'fictitious forces' that appear in moving non-inertial frames.

The surface of the macula closely resembles the interior section of a sphere. The displacement of the otoliths is detected by a vast population of hair cells lining the macula. This population of neural receptors robustly detect and transmit the otolith displacement information to the neural system [35–38]. Thus a spherical pendulum with concentrated mass, m, would be subjected to the same forces and to the same spherical motion constraints as are the otoliths. The provision of a damping term with coefficient, β, is required to model the viscous action of the endolymph liquid filling the saccule and utricle cavities. Finally, it is convenient to parametrise the relative

movement of the moving mass by two angles, θ_x and θ_y, since any other smooth parametrisation would leave our result unchanged. Because we assumed in our analysis that the otolith system operated under normal conditions, we did not attempt to include mechanical stops in our model in order to represent the limits of the pendulum's displacements.

(c) Notation

The formulation of the dynamical model crucially depends on several coordinate systems moving in relation to one another. Vector and tensorial quantities that are sensitive to the frame in which they are expressed have a left superscript to indicate it. The unit vectors of frames were already denoted this way. A rotation transformation is encoded by a matrix, ${}_{\mathbb{B}}\mathbf{R}_{\mathbb{A}} \in \mathcal{SO}(3)$, that transforms by left multiplication vectors expressed in a frame, $\mathbb{A}$, into vectors expressed in frame $\mathbb{B}$, e.g. ${}^{\mathbb{I}}\boldsymbol{g} = {}_{\mathbb{I}}\mathbf{R}_{\mathbb{H}}\,{}^{\mathbb{H}}\boldsymbol{g}$. Thus ${}_{\mathbb{B}}\mathbf{R}_{\mathbb{A}}$ expresses the orientation of $\mathbb{A}$ with respect to $\mathbb{B}$. Given an angular velocity vector, ${}^{\mathbb{B}}_{\mathbb{B}}\boldsymbol{\omega}_{\mathbb{A}} \in \mathcal{R}^3$, the symbol ${}^{\mathbb{B}}_{\mathbb{B}}\tilde{\boldsymbol{\omega}}_{\mathbb{A}} \in o(3)$ denotes the corresponding skew-symmetric matrix and $o(3)$ denotes the Lie algebra of the orthogonal group $\mathcal{O}(3)$.

(d) Dynamical Model Equations

The Newton-Euler equations can be used to efficiently describe the dynamics of the head-pendulum system. Beginning with the head, without loss of generality it is assumed that mass is symmetrically and uniformly distributed about its center. In addition, the influence of the pendulum on the head movements is disregarded since the mass of the otoliths can be considered to be negligibly small before the mass of the head. Expressing the moment of inertia tensor of the head in the body-fixed frame, ${}^{\mathbb{H}}\mathbf{J}_{\mathrm{H}}$, allows one to write the head orientation dynamics by differentiating the head's angular momentum, $\boldsymbol{h}_{\mathrm{H}}$, with respect to time,

$$\boldsymbol{h}_{\mathrm{H}} = {}^{\mathbb{H}}\mathbf{J}_{\mathrm{H}}\,{}^{\mathbb{H}}_{\mathbb{I}}\boldsymbol{\omega}_{\mathbb{H}},$$
$$\dot{\boldsymbol{h}}_{\mathrm{H}} = \frac{\mathrm{d}}{\mathrm{d}t}\left({}^{\mathbb{H}}\mathbf{J}_{\mathrm{H}}\,{}^{\mathbb{H}}_{\mathbb{I}}\boldsymbol{\omega}_{\mathbb{H}}\right) = {}^{\mathbb{H}}\mathbf{J}_{\mathrm{H}}\,{}^{\mathbb{H}}_{\mathbb{I}}\dot{\boldsymbol{\omega}}_{\mathbb{H}} + {}^{\mathbb{H}}_{\mathbb{I}}\boldsymbol{\omega}_{\mathbb{H}} \times {}^{\mathbb{H}}\mathbf{J}_{\mathrm{H}}\,{}^{\mathbb{H}}_{\mathbb{I}}\boldsymbol{\omega}_{\mathbb{H}},$$

where ${}^{\mathbb{H}}_{\mathbb{I}}\boldsymbol{\omega}_{\mathbb{H}}$ is the angular velocity of the head with respect to the inertial frame, $\mathbb{I}$, expressed in the body-fixed frame, $\mathbb{H}$. The dynamics of the head driven by a torque, ${}^{\mathbb{H}}\boldsymbol{\tau}$, is thus

$${}^{\mathbb{H}}\mathbf{J}_{\mathrm{H}}\,{}^{\mathbb{H}}_{\mathbb{I}}\dot{\boldsymbol{\omega}}_{\mathbb{H}} = -{}^{\mathbb{H}}_{\mathbb{I}}\boldsymbol{\omega}_{\mathbb{H}} \times {}^{\mathbb{H}}\mathbf{J}_{\mathrm{H}}\,{}^{\mathbb{H}}_{\mathbb{I}}\boldsymbol{\omega}_{\mathbb{H}} + {}^{\mathbb{H}}\boldsymbol{\tau}.$$

The torque, ${}^{\mathbb{H}}\boldsymbol{\tau} \in \mathcal{R}^3$, is produced by the neck muscles to orient the head with respect to the torso. The kinematics of the head rotations is

$${}_{\mathbb{I}}\dot{\mathbf{R}}_{\mathbb{H}} = {}_{\mathbb{I}}\mathbf{R}_{\mathbb{H}}\,{}^{\mathbb{H}}_{\mathbb{I}}\tilde{\boldsymbol{\omega}}_{\mathbb{H}},$$

where ${}^{\mathbb{H}}_{\mathbb{I}}\tilde{\boldsymbol{\omega}}_{\mathbb{H}}$ is the skew-symmetric matrix corresponding to the angular velocity of the head.

Because the mass representing the otoliths evolves in a moving frame, the dynamics that govern its motions is more complicated than that of the head since it must account for the 'fictitious forces' present in a non-inertial frame. It is also subject to the action of gravity and of viscous forces. Differentiating the angular momentum of the pendulum with respect to time and adding the other terms gives,

$$\begin{aligned}{}^{\mathbb{S}}\mathbf{J}_{\mathrm{S}}\,{}^{\mathbb{S}}_{\mathbb{I}}\dot{\boldsymbol{\omega}}_{\mathbb{S}} = &-\underbrace{m\,{}^{\mathbb{S}}\boldsymbol{l} \times {}_{\mathbb{S}}\mathbf{R}_{\mathbb{I}}\;{}_{\mathbb{I}}\mathbf{R}_{\mathbb{H}}\,{}^{\mathbb{H}}\boldsymbol{a}}_{\text{acceleration}} - \underbrace{{}^{\mathbb{S}}_{\mathbb{I}}\boldsymbol{\omega}_{\mathbb{S}} \times {}^{\mathbb{S}}\mathbf{J}_{\mathrm{S}}\,{}^{\mathbb{S}}_{\mathbb{I}}\boldsymbol{\omega}_{\mathbb{S}}}_{\text{gyroscopic}} \\ &+\underbrace{m\,{}^{\mathbb{S}}\boldsymbol{l} \times {}_{\mathbb{S}}\mathbf{R}_{\mathbb{I}}\,{}^{\mathbb{I}}\boldsymbol{g}}_{\text{gravity}} - \underbrace{\beta({}^{\mathbb{S}}_{\mathbb{I}}\boldsymbol{\omega}_{\mathbb{S}} - {}_{\mathbb{S}}\mathbf{R}_{\mathbb{I}}\;{}_{\mathbb{I}}\mathbf{R}_{\mathbb{H}}\,{}^{\mathbb{H}}_{\mathbb{I}}\boldsymbol{\omega}_{\mathbb{H}})}_{\text{damping}},\end{aligned}$$

where ${}^{\mathbb{S}}\mathbf{J}_{\mathrm{S}}$ is the pendulum's principal inertia tensor, ${}^{\mathbb{S}}_{\mathbb{I}}\boldsymbol{\omega}_{\mathbb{S}}$ is the angular velocity of the pendulum with respect to the inertial frame, ${}^{\mathbb{S}}\boldsymbol{l} = \begin{pmatrix}0 & 0 & l\end{pmatrix}^{\mathrm{T}}$ is the vector from the pivot of the pendulum to the center of its mass, ${}_{\mathbb{S}}\mathbf{R}_{\mathbb{I}}$, is the rotation matrix which defines the orientation of the pendulum

with respect to the inertial frame, while ${}^{\mathbb{H}}\boldsymbol{a} \in \mathcal{R}^3$ is the acceleration of center of mass of the head expressed in head coordinates. In addition there is a gravitational component associated to the acceleration ${}^{\mathbb{I}}\boldsymbol{g} = \begin{pmatrix} 0 & 0 & -9.81 \end{pmatrix}^{\mathrm{T}}$ and a damping term with coefficient β. The head and pendulum motions are thus coupled through damping and translational acceleration of the head. The pendulum kinematics is

$$ {}_{\mathbb{I}}\dot{\mathbf{R}}_{\mathbb{S}} = {}_{\mathbb{I}}\mathbf{R}_{\mathbb{S}}\, {}^{\mathbb{S}}_{\mathbb{I}}\tilde{\boldsymbol{\omega}}_{\mathbb{S}}. $$

When the head is stationary, the gravitational term and the damping term are the only terms remaining, and the pendulum aligns itself with the gravitational vertical.

Written in scalar form, these equations would cover several pages. For further analysis, the gyroscopic term for the pendulum dynamics can be reasonably assumed to be negligibly small because it is quadratic in angular velocities which can themselves be assumed to be small. Under these conditions, the relevant dynamics is expressed as a system of four coupled nonlinear equations,

$$ \begin{cases} {}^{\mathbb{S}}\mathbf{J}_{\mathrm{S}}\, {}^{\mathbb{S}}_{\mathbb{I}}\dot{\boldsymbol{\omega}}_{\mathbb{S}} = m\, {}^{\mathbb{S}}\boldsymbol{l} \times {}_{\mathbb{S}}\mathbf{R}_{\mathbb{I}}\, {}^{\mathbb{I}}\boldsymbol{g} - m\, {}^{\mathbb{S}}\boldsymbol{l} \times \underbrace{{}_{\mathbb{S}}\mathbf{R}_{\mathbb{I}}\, {}_{\mathbb{I}}\mathbf{R}_{\mathbb{H}}}_{{}_{\mathbb{S}}\mathbf{R}_{\mathbb{H}}}\, {}^{\mathbb{H}}\boldsymbol{a} - \beta({}^{\mathbb{S}}_{\mathbb{I}}\boldsymbol{\omega}_{\mathbb{S}} - \underbrace{{}_{\mathbb{S}}\mathbf{R}_{\mathbb{I}}\, {}_{\mathbb{I}}\mathbf{R}_{\mathbb{H}}}_{{}_{\mathbb{S}}\mathbf{R}_{\mathbb{H}}}\, {}^{\mathbb{H}}_{\mathbb{I}}\boldsymbol{\omega}_{\mathbb{H}}), \\ {}^{\mathbb{S}}\mathbf{J}_{\mathrm{S}}\, {}^{\mathbb{H}}_{\mathbb{I}}\dot{\boldsymbol{\omega}}_{\mathbb{H}} = {}^{\mathbb{H}}\boldsymbol{\tau}, \\ {}_{\mathbb{I}}\dot{\mathbf{R}}_{\mathbb{S}} = {}_{\mathbb{I}}\mathbf{R}_{\mathbb{S}}\, {}^{\mathbb{S}}_{\mathbb{I}}\tilde{\boldsymbol{\omega}}_{\mathbb{S}}, \\ {}_{\mathbb{I}}\dot{\mathbf{R}}_{\mathbb{H}} = {}_{\mathbb{I}}\mathbf{R}_{\mathbb{H}}\, {}^{\mathbb{H}}_{\mathbb{I}}\tilde{\boldsymbol{\omega}}_{\mathbb{H}}. \end{cases} \tag{2.1} $$

The otolith organs respond to the inclination of the head with respect to the gravitational vertical in the sagittal and in the coronal planes. The measurements correspond to the angles, θ_x and θ_y, between unit vector ${}^{\mathbb{S}}\boldsymbol{k}$ projected onto the sagittal and the coronal planes and the unit vector ${}^{\mathbb{H}}\boldsymbol{k}$. These projections can be expressed using the elements of rotations. Thus, the outputs of the system, z_1 and z_2, can also be written in terms of the tangent of the inclination angles of the pendulum in the sagittal and the coronal planes respectively,

$$ \begin{cases} z_1 \triangleq \tan\theta_x = \dfrac{\left[{}_{\mathbb{H}}\mathbf{R}_{\mathbb{S}}\right]_{\{3,2\}}}{\left[{}_{\mathbb{H}}\mathbf{R}_{\mathbb{S}}\right]_{\{3,3\}}}, \\ z_2 \triangleq \tan\theta_y = \dfrac{\left[{}_{\mathbb{H}}\mathbf{R}_{\mathbb{S}}\right]_{\{3,1\}}}{\left[{}_{\mathbb{H}}\mathbf{R}_{\mathbb{S}}\right]_{\{3,3\}}}, \end{cases} \tag{2.2} $$

where ${}_{\mathbb{H}}\mathbf{R}_{\mathbb{S}} = {}_{\mathbb{I}}\mathbf{R}_{\mathbb{H}}{}^{\mathrm{T}}\, {}_{\mathbb{I}}\mathbf{R}_{\mathbb{S}}$ and $[.]_{\{n,m\}}$ denotes the (n,m) entry of a matrix. When the state of system is known, the orientation of the head in inertial coordinates, described by angles Θ_x and Θ_y, is similarly given by the formulae,

$$ \tan\Theta_x = \frac{\left[{}_{\mathbb{I}}\mathbf{R}_{\mathbb{H}}\right]_{\{3,2\}}}{\left[{}_{\mathbb{I}}\mathbf{R}_{\mathbb{H}}\right]_{\{3,3\}}} \quad \text{and} \quad \tan\Theta_y = \frac{\left[{}_{\mathbb{I}}\mathbf{R}_{\mathbb{H}}\right]_{\{3,1\}}}{\left[{}_{\mathbb{I}}\mathbf{R}_{\mathbb{H}}\right]_{\{3,3\}}}. $$

if Θ_x and Θ_y are the angles between the unit vector ${}^{\mathbb{H}}\boldsymbol{k}$ projected onto the principal planes of the inertial coordinates and the vector ${}^{\mathbb{I}}\boldsymbol{k}$.

The outputs z_1 and z_2 for the system (2.2) can thus be thought to deliver an equivalent information as that given by the relative displacements of the otoliths in the biological vestibular system. In (2.1), these outputs evolve under the action of head rotations driven by the torque ${}^{\mathbb{H}}\boldsymbol{\tau}$, of the head translational movements represented by ${}^{\mathbb{H}}\boldsymbol{a}$, and of the ambient gravity field, ${}^{\mathbb{I}}\boldsymbol{g}$.

To put the system in state space form we define, $\boldsymbol{s} = \left\{ {}^{\mathbb{S}}_{\mathbb{I}}\boldsymbol{\omega}_{\mathbb{S}}, {}^{\mathbb{H}}_{\mathbb{I}}\boldsymbol{\omega}_{\mathbb{H}}, {}_{\mathbb{I}}\mathbf{R}_{\mathbb{S}}, {}_{\mathbb{I}}\mathbf{R}_{\mathbb{H}} \right\} \in \mathcal{R}^{24}$, a state vector where the elements of the vectors and matrices populate a single vector. The system can

then be written in state space form,

$$\Xi(\boldsymbol{s},\boldsymbol{r}) \equiv \begin{cases} \dot{\boldsymbol{s}} = \boldsymbol{v}(\boldsymbol{s},\boldsymbol{r}), \\ \boldsymbol{z} = \boldsymbol{o}(\boldsymbol{s}), \end{cases} \tag{2.3}$$

where $\boldsymbol{r} = \begin{pmatrix} {}^{\mathbb{H}}\boldsymbol{\tau} & {}^{\mathbb{H}}\boldsymbol{a} \end{pmatrix}^{\mathrm{T}} \in \mathcal{R}^6$ is treated as an aggregated input and where the output is $\boldsymbol{z} = \begin{pmatrix} z_1 & z_2 \end{pmatrix}^{\mathrm{T}} \in \mathcal{R}^2$. The equations of the system model written in this form are linearly dependent since the rotation matrices are members of $\mathcal{SO}(3)$, leaving twelve of the state equations to be independent. It is important to note that the choice of expressing the state dynamics through rotation matrices ensures a unique and global system representation [39]. All the functions in the state space representation, Ξ, are rational, that is, all the components of $\boldsymbol{v}$ and $\boldsymbol{o}$ are ratios of polynomials in $\boldsymbol{s}$ and $\boldsymbol{r}$.

(e) Head Stabilisation

To control the head, we adopted the three-dimensional stabilising control law proposed by Chaturvedi et al. [39]. With this feedback, the torque applied to the head was

$${}^{\mathbb{H}}\boldsymbol{\tau}_{\mathrm{s}}(\boldsymbol{s}) \equiv \mathbf{K}_{\mathrm{p}}\,\boldsymbol{\Omega} - \mathbf{K}_{\mathrm{d}}\,{}^{\mathbb{H}}_{\mathbb{I}}\boldsymbol{\omega}_{\mathbb{H}}, \tag{2.4}$$

where $\mathbf{K}_{\mathrm{p}}$, $\mathbf{K}_{\mathrm{d}} \in \mathcal{R}^{3\times 3}$ are positive definite matrices; and where $\boldsymbol{s}$ is the state of the system as defined previously. The vector $\boldsymbol{\Omega} \in \mathcal{R}^3$ is defined by

$$\boldsymbol{\Omega} = \sum_{i=1}^{3} e_i \times (\mathbf{I}\,{}_{\mathbb{I}}\mathbf{R}_{\mathbb{H}}\,e_i),$$

with $\mathbf{I} = \begin{pmatrix} e_1 & e_2 & e_3 \end{pmatrix}$ the identity matrix. This control law comprises proportional and derivative feedback control structure and it can be interpreted as introducing a potential though the attitude-dependent term and dissipation through the angular-velocity-dependent term [39]. The objective of the controller is to asymptotically stabilise the head orientation, ${}_{\mathbb{I}}\mathbf{R}_{\mathbb{H}}$, to achieve the upright orientation, i.e. the identity rotation matrix, $\mathbf{I}$. It can be shown that this global control law is able to asymptotically stabilise a rigid body constraint by a spherical pivot [39]. The acceleration of the head, ${}^{\mathbb{H}}\boldsymbol{a}$, has no influence on this result since the dynamics that govern the motion of the head is decoupled from that of the pendulum.

(f) Nonlinear algebraic observability

To clarify the notion of parameter identifiability in nonlinear systems, it is useful to step back and consider a standard system representation,

$$\Sigma(\boldsymbol{x},\boldsymbol{u},\boldsymbol{p}) \equiv \begin{cases} \dot{\boldsymbol{x}} = \boldsymbol{f}(\boldsymbol{x},\boldsymbol{u},\boldsymbol{p}), \quad \boldsymbol{x}(t_0) = \boldsymbol{x}_0, \\ \dot{\boldsymbol{p}} = 0, \qquad\qquad\qquad\qquad t \geq t_0 \\ \boldsymbol{y} = \boldsymbol{g}(\boldsymbol{x},\boldsymbol{u},\boldsymbol{p}), \end{cases}$$

where $\boldsymbol{x}(t) \in \mathcal{R}^n, \boldsymbol{u}(t) \in \mathcal{R}^m, \boldsymbol{y}(t) \in \mathcal{R}^r, \boldsymbol{p} \in \mathcal{R}^p$, for $t \geq t_0$. The functions $\boldsymbol{f}$ and $\boldsymbol{g}$ are algebraic in the variables $\boldsymbol{x}, \boldsymbol{u}, \boldsymbol{p}$. The vectors $\boldsymbol{x}_0$ and $\boldsymbol{p}_0$ represent initial conditions of the system at time t_0. The quantity $\boldsymbol{p}$ represents parameters which do not vary with time.

If the $\boldsymbol{f}$ and $\boldsymbol{g}$ are are differentiable sufficiently many times, if $\boldsymbol{u}^{(k)}$ and $\boldsymbol{y}^{(l)}$ denote the k-th and l-th derivatives of $\boldsymbol{u}$ and $\boldsymbol{y}$, and if $\mathcal{N}$ is the set of natural numbers, a simplified definition of observability is,

Definition 1 (Algebraic Observability). *For a given value of parameter $\boldsymbol{p}$, Σ is algebraically observable if the initial values of inputs and outputs and their derivatives of any order, i.e. $\boldsymbol{u}(t_0)$, $\boldsymbol{y}(t_0)$, and $\boldsymbol{u}^{(k)}(t_0)$, $\boldsymbol{y}^{(l)}(t_0)$, $k, l \in \mathcal{N}$, determine uniquely the initial state, $\boldsymbol{x}_0$.*

Rigorous conditions for algebraic observability were stated by Diop and Fliess in [40]. Later, the notion of algebraic observability was found to be almost equivalent to the differential geometric observability developed by Herman and Krener [41], [42]. Parameter identifiability is defined similarly.

Definition 2 (Algebraic Parameter Identifiability)**.** *The parameter $\boldsymbol{p}$ of Σ is algebraically identifiable if the initial values of its inputs and outputs and their derivatives of any order, i.e. $\boldsymbol{u}(t_0)$, $\boldsymbol{y}(t_0)$, and $\boldsymbol{u}^{(k)}(t_0)$, $\boldsymbol{y}^{(l)}(t_0)$, $k, l \in \mathcal{N}$, uniquely determine $\boldsymbol{p}$.*

Because the systems considered are nonlinear, these definitions refer to local observability and identifiability which allow for the existence of multiple values of $\boldsymbol{x}_0$ or $\boldsymbol{p}_0$ determined from $\boldsymbol{u}(t_0)$, $\boldsymbol{y}(t_0)$, $\boldsymbol{u}^{(k)}(t_0)$, $\boldsymbol{y}^{(l)}(t_0)$, $k, l \in \mathcal{N}$, but only if these multiple values are *isolated*, i.e. are separated by distance. A simple illustrative example on nonlinear system identifiability and observability can be found in [43].

(g) Application to the head-otolith system

Although the head system $\Xi(\boldsymbol{s}, {}^{\mathbb{H}}\boldsymbol{\tau}, {}^{\mathbb{H}}\boldsymbol{a})$ satisfies the assumptions for applicability of the algebraic observability analysis, it is so heavily nonlinear and highly dimensional that explicit observability analysis is infeasible as the number of terms and their degree would explode combinatorially with the eleven successive derivations required by the analysis of (2.3). We are not aware of any computer algebra systems capable of solving systems of rational equations of such size.

Luckily, semi-numerical probabilistic computer algorithms were developed to serve such cases. The software package developed by Sedoglavic is the most prominent representative of such algorithms [43]. The core algorithm is implemented in Maple™ and has previously been employed to test identifiability of biological and other complex systems [44–46]. The semi-numerical approach developed by Sedoglavic was employed to test observability and identifiably of the system $\Xi(\boldsymbol{s}, {}^{\mathbb{H}}\boldsymbol{\tau}, {}^{\mathbb{H}}\boldsymbol{a})$ with probability exceeding 0.99.

Eight cases were tested, see Table 1. They corresponded to instances that would be relevant to a locomoting organism. Cases 1-4 in Table 1 represent the scenarios when the head was not accelerated while the remaining cases 5-8 assume that the head was accelerated. Part of the input, ${}^{\mathbb{H}}\boldsymbol{\tau}$ or ${}^{\mathbb{H}}\boldsymbol{a}$, could be assumed to be unknown. The input torque could be zero; an unknown constant value, ${}^{\mathbb{H}}\tilde{\boldsymbol{\tau}}_{\mathrm{C}}$, independent from the state; a known time-varying value, ${}^{\mathbb{H}}\boldsymbol{\tau}(t)$; or a stabilising control, ${}^{\mathbb{H}}\boldsymbol{\tau}_{\mathrm{s}}(\boldsymbol{s})$ according to the law (2.4). Similarly, the input acceleration could be zero, or an unknown constant, ${}^{\mathbb{H}}\tilde{\boldsymbol{a}}_{\mathrm{C}}$.

First, we tested whether the full system state, including head orientation, was observable, depending on the head orientation control by torque input. For example, the last case of Table 1 was when the head was stabilised by the state feedback while being accelerated, whereas the first case is when it was left tumbling out of control at constant translational velocity. Similarly, to the last case, the head orientation was observable in case 4 when it was stabilised by the state feedback. The head orientation was not observable when unknown torque was applied, case 2, or the applied torque was known but state independent, case 3 (non-stabilised head). Same results were observed for the cases when the head was accelerated: the head orientation was not observable when input torque was unknown, case 6, or known but state independent, case 7.

It is seen that the orientation of the head in inertial coordinates is observable only when the head is stabilised, cases 4 and 8, because the algebraic structure of the system is positively altered by the application of a stabilising feedback. Secondly, acceleration was tested for identifiability. The identifiability of the translational acceleration of the head is possible only when the torque is known or when it results from a known feedback law, cases 7 and 8. That means that the head's translational acceleration can be reconstructed in the model when the head is stabilised with the state feedback controller.

Table 1. Cases tested for observability and identifiability.

	Head torque	System	Observability	Identifiability
non-accelerated head:				
1	no input	$\Xi\left[\boldsymbol{x},(0,0)\right]$	negative	–
2	unknown torque	$\Xi\left[\boldsymbol{x},\left({}^{\mathbb{H}}\tilde{\boldsymbol{\tau}}_{\mathrm{C}},0\right)\right]$	negative	–
3	known torque	$\Xi\left[\boldsymbol{x},\left({}^{\mathbb{H}}\boldsymbol{\tau}(t),0\right)\right]$	negative	–
4	stabilising torque	$\Xi\left[\boldsymbol{x},\left({}^{\mathbb{H}}\boldsymbol{\tau}(\boldsymbol{x}),0\right)\right]$	positive	–
accelerated head:				
5	no input	$\Xi\left[\boldsymbol{x},\left(0,{}^{\mathbb{H}}\tilde{\boldsymbol{a}}_{\mathrm{C}}\right)\right]$	negative	negative
6	unknown torque	$\Xi\left[\boldsymbol{x},\left({}^{\mathbb{H}}\tilde{\boldsymbol{\tau}}_{\mathrm{C}},{}^{\mathbb{H}}\tilde{\boldsymbol{a}}_{\mathrm{C}}\right)\right]$	negative	negative
7	known torque	$\Xi\left[\boldsymbol{x},\left({}^{\mathbb{H}}\boldsymbol{\tau}(t),{}^{\mathbb{H}}\tilde{\boldsymbol{a}}_{\mathrm{C}}\right)\right]$	negative	positive
8	stabilising torque	$\Xi\left[\boldsymbol{x},\left({}^{\mathbb{H}}\boldsymbol{\tau}(\boldsymbol{x}),{}^{\mathbb{H}}\tilde{\boldsymbol{a}}_{\mathrm{C}}\right)\right]$	positive	positive

(h) Discussion

The results described in Table 1 support the hypothesis H_1. Sedoglavic's algorithm could detect the algebraic observability of $\Xi\left[\boldsymbol{x},\left({}^{\mathbb{H}}\boldsymbol{\tau}(\boldsymbol{x}),0\right)\right]$ or $\Xi\left[\boldsymbol{x},\left({}^{\mathbb{H}}\boldsymbol{\tau}(\boldsymbol{x}),{}^{\mathbb{H}}\tilde{\boldsymbol{a}}_{\mathrm{C}}\right)\right]$, that is, only when stabilising state-feedback was employed, but did not provide any method for the actual reconstruction or estimation of the state, $\boldsymbol{x}$, a crucial part of which is the rotation matrix, ${}_{\mathbb{I}}\mathbf{R}_{\mathbb{H}}$.

Such method can appeal to a number of approaches, including nonlinear observers, such as differential algebraic observers based on numerical differentiation of the output, or some kind of particle filter based on a Markov chain, or simply an extended Kalman filter employing local linearisation of the system.

Although there are results guaranteeing the local convergence of the extended Kalman filter, such results hold only for a very special class of systems and the region of observer convergence is usually estimated from Monte Carlo simulations. Furthermore, since the system Ξ is heavily nonlinear, in all likelihood, the separation principle does not apply here with the unfortunate consequence that the addition of an observer may destabilise an otherwise stable control. The opposite is also possible, that the control could upset the convergence of a well-designed observer. In the nonlinear case, separation principle results are scarce [47], unlike for linear systems for which it suffices to ensure that the eigenvalues of the controlled system do not interfere with the eigenvalues of the observed system.

This observation suggests an additional important advantage of the head stabilisation strategy during movement. As the orientation of the head approaches the upright position, the linearisation of the head-otolith system becomes a better approximation of the original nonlinear system. As a result, computationally inexpensive linear controllers and observers can be expected to perform just as well, if not better, than computationally complex nonlinear controllers and observers, which in the case of an animal, would be metabolically costly. In the following section we demonstrate the convergence of simultaneous stabilisation and observation tasks assuming that head upright orientation and movements in the sagittal plane allow linear modelling of the head-otolith system.

3. Resolution of the acceleration-tilt ambiguity

(a) Movements in the sagittal plane

We demonstrate how the head upright head stabilisation strategy leads to significant system simplification that enables us to model verticality estimation and head stabilisation control

as linear systems. Theoretical results presented in the previous section has demonstrated that complex head-otolith systems become fully observable with state feedback stabilisation control of the head. In the following we demonstrate the importance of head stabilisation behaviour for gravito-inertial resolution with the help of linear control theory. We demonstrate that linearisation is crucial to maintain a simple internal model and it is applicable to normal locomotion scenario, i.e. locomotion with head stabilisation in the sagittal plane.

Planar movements of the head are behaviourally relevant in their own right (walking, running, riding) but also enable the resolution of the acceleration-tilt ambiguity using information arising exclusively from the head/otolith model system, Ξ. The spatial case would also be feasible but would be considerably more involved algebraically and, as discussed above, computationally. In the sagittal plane, the rotation matrices for the head and the pendulum take the form,

$$
{}_{\mathbb{H}}\mathbf{R}_{\mathbb{S}} = \begin{pmatrix} 1 & 0 & 0 \\ 0 & & \\ 0 & & {}_{\mathbb{H}}\bar{\mathbf{R}}_{\mathbb{S}} \end{pmatrix} = \begin{pmatrix} 1 & 0 & 0 \\ 0 & s_1 & s_2 \\ 0 & s_3 & s_4 \end{pmatrix},
$$

$$
{}_{\mathbb{I}}\mathbf{R}_{\mathbb{H}} = \begin{pmatrix} 1 & 0 & 0 \\ 0 & & \\ 0 & & {}_{\mathbb{I}}\bar{\mathbf{R}}_{\mathbb{H}} \end{pmatrix} = \begin{pmatrix} 1 & 0 & 0 \\ 0 & h_1 & h_2 \\ 0 & h_3 & h_4 \end{pmatrix},
$$

and the overall system dynamics reduces to

$$
\begin{cases}
J_{\mathrm{S}}\,\dot{\omega}_{\mathrm{S}} = m \begin{bmatrix} 0 \\ l \end{bmatrix} \times {}_{\mathbb{S}}\bar{\mathbf{R}}_{\mathbb{I}} \begin{bmatrix} 0 \\ -g \end{bmatrix} - m \begin{bmatrix} 0 \\ l \end{bmatrix} \times {}_{\mathbb{S}}\bar{\mathbf{R}}_{\mathbb{I}}\, {}_{\mathbb{I}}\bar{\mathbf{R}}_{\mathbb{H}}{}^{\mathbb{H}} \begin{bmatrix} a_y \\ a_z \end{bmatrix} \\
\qquad\qquad - \beta \left(\omega_{\mathrm{S}} - {}_{\mathbb{S}}\bar{\mathbf{R}}_{\mathbb{I}}\, {}_{\mathbb{I}}\bar{\mathbf{R}}_{\mathbb{H}}\, \omega_{\mathrm{H}} \right), \\
J_{\mathrm{H}}\,\dot{\omega}_{\mathrm{H}} = \tau, \\
{}_{\mathbb{I}}\dot{\bar{\mathbf{R}}}_{\mathbb{S}} = {}_{\mathbb{I}}\bar{\mathbf{R}}_{\mathbb{S}} \begin{pmatrix} 0 & -\omega_{\mathrm{S}} \\ \omega_{\mathrm{S}} & 0 \end{pmatrix} \\
{}_{\mathbb{I}}\dot{\bar{\mathbf{R}}}_{\mathbb{H}} = {}_{\mathbb{I}}\bar{\mathbf{R}}_{\mathbb{H}} \begin{pmatrix} 0 & -\omega_{\mathrm{H}} \\ \omega_{\mathrm{H}} & 0 \end{pmatrix}.
\end{cases}
\tag{3.1}
$$

with $\dot{\omega}_{\mathrm{S}}$ and $\dot{\omega}_{\mathrm{H}}$ representing the angular velocities of the pendulum and the head in the sagittal plane respectively. The entries of the matrices ${}_{\mathbb{I}}\bar{\mathbf{R}}_{\mathbb{H}}$ and ${}_{\mathbb{S}}\bar{\mathbf{R}}_{\mathbb{H}}$ satisfy $h_1 = h_4$, $h_2 = -h_3$, $s_1 = s_4$, and $s_2 = -s_3$. Within a neighbourhood of the upright position, the small-angle approximation of the dynamics around the vertical orientation, with $\Theta_x \simeq h_3$ and $\theta_x \simeq s_3$, yields a fourth-order system,

$$
\begin{cases}
J_{\mathrm{S}}\,\dot{\omega}_{\mathrm{S}} = -m\,l\,g\,(\theta_x + \Theta_x) + m\,l\,a_y - \beta(\omega_{\mathrm{S}} - \omega_{\mathrm{H}}), \\
J_{\mathrm{H}}\,\dot{\omega}_{\mathrm{H}} = \tau,
\end{cases}
$$

Denoting the stacked state vector of the system by x, the linearised system can be written in canonical form,

$$
\dot{x} = Ax + B\tau.
$$

The three-dimensional head stabilising control boils down to angular PD control,

$$
\tau_x = -k_p\,\Theta_x - k_d\,\dot{\Theta}_x \triangleq Kx. \tag{3.2}
$$

The output measurement which corresponds to the otolith's response becomes,

$$
y = \Theta_x + \theta_x \triangleq Cx \tag{3.3}
$$

A standard linear control-observer pair, [48], can now be employed to carry out the task of verticality estimation. Such system is written,

$$
\dot{\hat{x}} = A\hat{x} + BKx + L(y - C\hat{x}), \tag{3.4}
$$

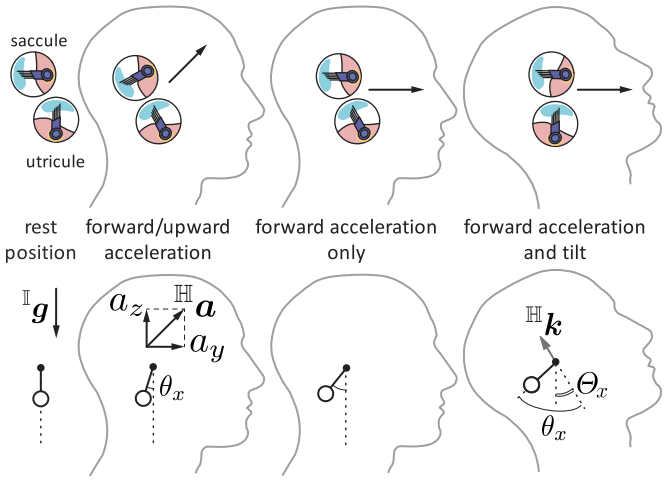

Figure 2. Illustration of the equivalence between the vestibular system and the pendulum model with regard to the sensory ambiguities. The first and the last cases correspond to indistinguishable sensory inputs.

where $\hat{x}$ is the estimated state, y is the output measurement, and L the observer gain. According to the separation principle applicable to linear systems, the above controller and observer can be employed within the same feedback loop where they will not interfere with one another.

(b) Relationship with motion illusions

It is now shown by simulation that the linearised model can be employed to resolve the so-called acceleration/tilt ambiguity [49].

Before, it is useful to refer to Fig. 2 to gain an intuitive understanding of the origin of this ambiguity. In the first column, when a head is accelerated forward and upward simultaneously, the saccule and the utricle, as they should, both give a signal arising from the deflection of the otoliths from their resting position. When the head is accelerated forward, second column, the utricle gives a signal but not the saccule. In the third column, an upward tilt of the head causes the acceleration of gravity to influence strongly the otoliths sending a signal to the brain that can be interpreted as the head being accelerated upward as in the first column. The second row of Fig. 2 emphasises again the point made earlier that a pendulum oscillating freely in a non-inertial frame captures the essential properties of any inertial measurement system because all depend on the same universal laws of movement, regardless of the constraints introduced by their practical realisations.

When the head of system Ξ is tilted by an angle Θ_x while being accelerated, the acceleration-tilt ambiguity can be modelled by a single constraint with two unknowns,

$$a_y = g\sin(\theta_x - \Theta_x).$$

Thus, in order to access acceleration, a_y, the knowledge of head tilt, Θ_x, is required, and conversely.

When the head of system Ξ is in the neighbourhood of the upright position, the pendulum responds to linear accelerations following,

$$g\tan\theta_x = a_y. \tag{3.5}$$

By analogy, if a head is in the neighbourhood of the upright position, the otolith organs reports translational accelerations directly. An ambiguity, termed gravito-inertial [50], arises during steady acceleration and when the head angular velocity is constant since the single constraint, (3.5), has two unknowns.

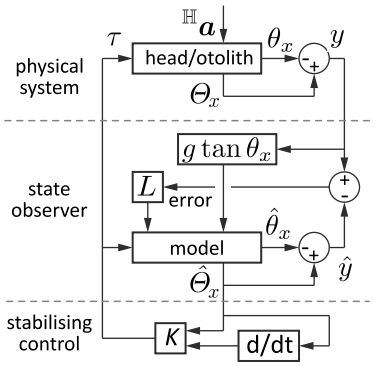

Figure 3. Control diagram used in the simulations corresponding to the full nonlinear system, (3.1), the simplified control (3.2), the output equation (3.3), the simplified observer (3.4), and the nonlinear correction (3.5).

Additional information may be obtained from other sensory inputs or from prior information. A good candidate for these other sensory inputs, besides vision of course, is the angular velocity information supplied by the semicircular canals. It is well known, however, that orientation confusions during motion persist in many cases. In flight simulators, for instance, where they can be leveraged to simulate ascensional acceleration by tilting the cabin while maintaining the visual input fixed relative to the viewer. These occurrences are consistent with our earlier observation that the availability of angular rate information has no influence upon the lack of observability of head orientation in space. Perceptual ambiguities during motion have been the subject of numerous studies, e.g. [51–59].

(c) Numerical Simulations

The premise of our study rested on the hypothesis that active feedback control of the head orientation using idiothetic information only modified profoundly the capacity of the nervous system to estimate the vertical in the presence of perturbations caused by body movements. The diagram in Fig. 3 was used for the numerical simulations. It represents the verticality estimator and head stabilisation control in the sagittal plane developed in Section 3(a). The physical system which represents the coupled head-otolith dynamics in sagittal plane modelled with (3.1) has two inputs, the torque applied to the head, $\tau = \tau_x$, and the unknown linear acceleration with components a_y and a_z. The linear acceleration is assumed to be unknown and its reconstruction is used as described below. The physical system has two outputs, the unknown head absolute inclination in the sagittal plane w.r.t. the vertical, Θ_x, and the measured angular displacement of the pendulum relative to the head, θ_x. The observer which estimates the head orientation with respect to the vertical in the sagittal plane is implemented based on (3.4) and assuming that (3.5) is valid for the upright head stabilisation. The stabilisation control is defined with (3.2). On that account, this case corresponds to the last row of Table 1.

The fidelity of the acceleration reconstruction depends on the quality of the estimation of the head tilt as a function of the tuning of the observer and controller gains, L and K. This scheme is nevertheless able to resolve the motion ambiguities described earlier as a natural outcome of head stabilisation relative to the true vertical.

The parameters of the model were chosen to represent the critically damped behaviour of human otoliths with a natural frequency of 300 Hz [60]. The moment of inertia of the head was set at 0.0174 kg·m^2 which, is an average value found in human biomechanics studies [61].

A standard linear observer-controller pair was implemented, but to make the simulation as realistic as possible, the full nonlinear model of the head and of the otoliths system was used to simulate the physical system driven with a full set of inputs. In two simulation conditions, we

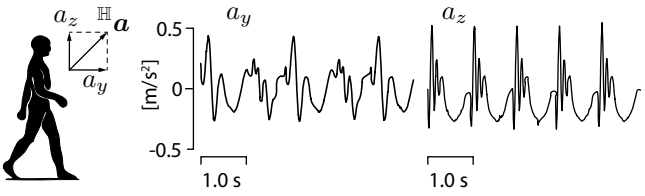

Figure 4. Typical acceleration of the human when walking.

investigated the performance of head angular orientation controller and observer during walking. The unknown to the observer-controller input linear acceleration of the head during walking in sagittal plane, Fig. 4, was obtained from human walking experiments [62].

In a first set of conditions, **a**, we tested how the controller-observer pair performed when it was required to control the head around different orientations. They were set at zero (upright position), ten, twenty-five, and forty degrees. The initial head tilt was set at five degrees in all cases. Thus, it was like trying to walk with the head upright or looking up at increasingly sharp angles.

In a second set of conditions, **b**, we tested how the controller-observer pair performed when it was required to stabilise the head around the zero degree orientation. This time, there were different initial orientations set at five, twenty, thirty and forty degrees.

In all cases, the head translational acceleration was not known to the controller-observer system. It was estimated and the corrected value, (3.5), was supplied to the computational model used by the state observer.

(d) Results

Figures 5a and 5b report the results for the different set-point orientations and for the different initial conditions, respectively. The upper panels reports the time history of head tilt in black lines and its estimated values in grey lines. The middle panels show the evolution of the estimation error for the various set-points and initial conditions. The lower panels show the actual head acceleration in black lines and the estimates in grey lines.

The overall results vindicate the previously derived theoretical results that predicted that estimation of the head orientation was possible only when the head stabilisation is achieved, in which case both the controller and the observer converge. It is when the set-point is zero and when the initial conditions are not exaggeratedly far from the upright position. Overall, the coupled observer-controller system operates correctly only when the reference angular orientation of the head is set to angles close to upright orientation of the head.

When the controller is asked to stabilise the head to an orientation which is far from the upright position, even for a tilt of ten degrees, the observer failed to provide proper estimates for the controller and the overall system diverged. When the initial condition was too far from the upright condition, the system also diverged. On the other hand, the head acceleration was correctly estimated when the head angular orientation was close to the upright position.

These simulation results support our second hypothesis, H_2. The head upright stabilisation enabled the application of a simplified linear model for coupled state estimation and control that could provide stable verticality information during locomotion.

(e) Discussion

While the results of Section 2 demonstrated that the overall head-otolith system became observable when the head was stabilised, the simulation results presented in this section further extend our contribution. For the planar locomotion case, we could demonstrate that upright head stabilisation control enabled model linearisation and facilitated gravito-inertial ambiguity

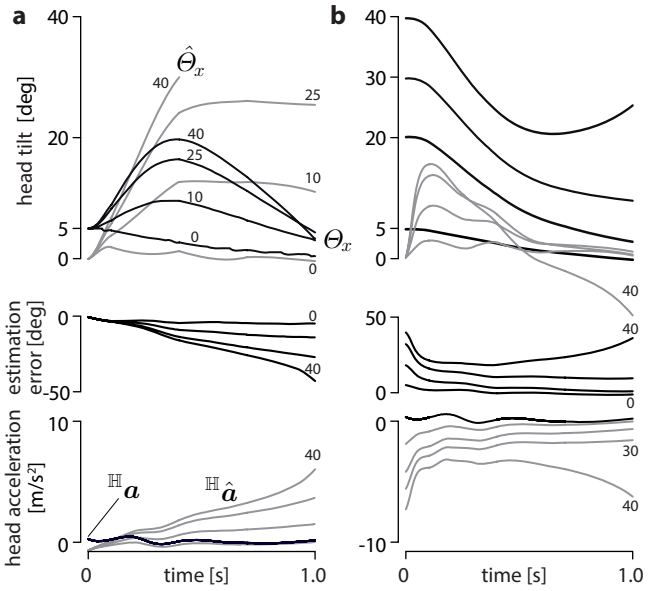

Figure 5. Simulation results. Upper panels: time history of head tilt. Middle panels: Estimation error. Lower panels: Time history of head acceleration. Left panels: different head orientation set-points. Right panels: different different initial conditions. Estimates are indicated in grey.

resolution through the observation that the otolith organs acted as translational acceleration sensors.

The lack of convergence of the observer-controller pair can be explained by two key factors. First, the simplified linear observation and control, and the attending separation principle, are not valid for large angles when the non-linear properties of the system become significant. Second, erroneous acceleration estimates render the gravito-inertial model ineffective, leading to incorrect overall estimates.

The results indicate that the overall system is stable (i.e. functional) only when the head is actively controlled to remain close to the upright configuration. It is then that a linearised model approximation becomes valid. This finding provides a potential explanation for the role of head stabilisation behaviour observed in animals and humans. These results also mirror the observation that in natural conditions humans and animals universally tend to maintain their head upright during a wide range of range of tasks and manoeuvres, thus facilitating the fusion of information arising from vestibular, visual, proprioceptive, and tactile inputs in a uniform earth-related frame of reference.

4. Conclusion

A mechanistic model of the head/otolith-organ system was used to analyse the fundamental property of observability of orientation in space, which to our knowledge was not considered before. Because the otolith organ, has clearly evolved to provide animals with the notion of verticality during movement, observability properties are essential. This model may appear simplistic compared to the actual biological systems but it has the advantage over previous models to capture a greater amount of the basic features of inertial sensors by accounting for the three-dimensional dynamics taking place in non-inertial frames, even if the gyroscopic terms were neglected. From inertial measurements only, orientation in space was found to be an unobservable quantity and thus no estimator could ever provide accurate, unbiased estimates for it.

Further analysis, presented in section 2, led to a remarkable result which supported the first hypothesis, H_1, namely, that a stabilising feedback law based on estimates of an unknown orientation could transform it into an observable quantity. This phenomenon is entirely owed to the highly nonlinear nature of non-inertial frame mechanics. In the theory of nonlinear systems, there is almost no result concerning similar occurrences, practically or theoretically, which makes it a candidate for further studies. As an additional point, in linear systems analysis it is easy to show that feedback cannot modify the observability properties of a system. Our result may therefore be seen as tribute to nature's inventiveness.

The construction of nonlinear observers can be hard and computationally very costly. A by-product of our finding is that the aforementioned stabilisation strategy makes it possible to not only estimate an unknown acceleration but, what is more, to do so using a linear observer, which supports the second hypothesis, H_2. This approach, which is described in Section 3, is considerably less costly than employing a nonlinear observer and is probably a more robust approach. Our results can apply to both biological or man-made systems, e.g. for autonomous locomotion [63–67] or robotics for gait and balance assistance [68,69], with the need to navigate in the absence of external references other than the ambient gravity field.

Ethics. This work did not involve any experimental work with human-subjects or animals, but only computer simulations and analysis of biological systems.

Data Accessibility. This article has no additional data.

Authors' Contributions. I.F., V.H. and H.M. conceived the mathematical models. All authors interpreted the computational results, and wrote the paper. IF implemented and performed most of the simulations. All authors gave final approval for publication.

Competing Interests. We have no competing interests.

Funding. I.F. was supported by a fellowship from Ecole Doctorale SMAER UPMC Paris Sorbonne University and by the European Research Council ERC Advanced Grant (PATCH no. 247300) to V.H. and in part by the EU FP7 grant BALANCE ICT-601003.

Acknowledgements. We thank Etienne Burdet, Jean-Paul Laumond and all reviewers for comments and thoughtful suggestions.

References

1. Hain TC, Ramaswamy TS, Hilmann MA. 2007 1. In *Anatomy and physiology of vestibular system,*. Philadelphia, PA: FA Davis Company 2 edition.
2. Angelaki DE, Dickman JD. 2003 Gravity or translation: Central processing of vestibular signals to detect motion or tilt. *Journal of Vestibular Research* **13**.
3. Vingerhoets RAA, De Vrijer M, Van Gisbergen JAM, Medendorp WP. 2009 Fusion of visual and vestibular tilt cues in the perception of visual vertical. *J Neurophysiol.* **101**, 1321–33.
4. Golding JF, Markey HM. 1996 Effect of frequency of horizontal linear oscillation on motion sickness and somatogravic illusion. *Aviation, space, and environmental medicine* **67**, 121–126.
5. Bisdorff AR, Wolsley CJ, Anastasopoulos D, Bronstein AM, Gresty MA. 1996 The perception of body verticality (subjective postural vertical) in peripheral and central vestibular disorders. *Brain* **119**, 1523–1534.
6. Yelnik AP. 2002 Perception of verticality after recent cerebral hemisphericstroke. *Stroke* **33**, 2247–2253.
7. Baker J, Goldberg J, Peterson B. 1985 Spatial and temporal response properties of the vestibulocollic reflex in decerebrate cats. *J Neurophysiol* **54**, 735–756.
8. Dieterich M, Brandt T. 1995 Vestibulo-ocular reflex. *Current opinion in neurology* **8**, 83–8.
9. Wilson VJ, Boyle R, Fukushima K, Rose PK, Shinoda Y, Sugiuchi Y, Uchino Y. 1995 The vestibulocollic reflex. *Journal of Vestibular Research : Equilibrium & Orientation* **5**, 147–170.
10. Money KE, Correia MJ. 1972 The vestibular system of the owl. *Comparative Biochemistry and Physiology Part A: Physiology* **42**, 353–358.
11. Frost BJ. 1978 The optokinetic basis of head-bobbing in the pigeon. *J Exp Biol.* **74**, 187–195.
12. Fuller JH, Maldonado H, Schlag J. 1983 Vestibular-oculomotor interaction in cat eye-head

movements. *Brain Research* **271**, 241–250.
13. Fuller JH. 1985 Eye and head movements in the pigmented rat. *Vision Research* **25**, 1121–1128.
14. Fuller JH. 1981 Eye and head movements during vestibular stimulation in the alert rabbit. *Brain Research* **205**, 363–381.
15. Guitton D, Kearney RE, Wereley N, Peterson BW. 1986 Visual, vestibular and voluntary contributions to human head stabilization. *Experimental Brain Research* **64**.
16. Davies MNO, Green PR. 1988 Head-bobbing during walking, running and flying: relative motion perception in the pigeon. *J Exp Biol.* **138**, 71–91.
17. Buchanan JJ, Horak FB. 2002 Vestibular loss disrupts control of head and trunk on a sinusoidally moving platform. *Journal of vestibular research : equilibrium & orientation* **11**, 371–89.
18. Pozzo T, Berthoz A, Lefort L. 1990 Head stabilisation during various locomotor tasks in humans. *Experimental Brain Research* **82**, 97–106.
19. Pozzo T, Berthoz A, Lefort L, Vitte E. 1991 Head stabilization during various locomotory tasks in humans II. Patients with bilateral vestibular deficits. *Experimental Brain Research* **85**, 208–217.
20. Winter DA. 1995 Human balance and posture control during standing and walking. *Gait & Posture* **3**, 193–214.
21. Pozzo T, Levik Y, Berthoz A. 1995 Head and trunk movements in the frontal plane during complex dynamic equilibrium tasks in humans. *Experimental Brain Research* **106**, 327–338.
22. Bronstein AM. 1998 Evidence for a Vestibular Input Contributing to Dynamic Head Stabilization in Man. *Acta oto-laryngologica* **105**, 1–6.
23. Green PR. 1998 Head orientation and trajectory of locomotion during jumping and walking in domestic chicks. *Brain, behavior and evolution* **51**, 48–58.
24. Troje NF, Frost BJ. 2000 Head-bobbing in pigeons: how stable is the hold phase?. *J Exp Biol.* **203**, 935–940.
25. Katzir G, Schechtman E, Carmi N, Weihs D. 2001 Head stabilization in herons. *Journal of Comparative Physiology A: Sensory, Neural, and Behavioral Physiology* **187**, 423–432.
26. Fujita M. 2003 Head bobbing and the body movement of little egrets (Egretta garzetta) during walking. *Journal of comparative physiology* **189**, 53–8.
27. Dunbar DC, Badam GL, Hallgrímsson B, Vieilledent S. 2004 Stabilization and mobility of the head and trunk in wild monkeys during terrestrial and flat-surface walks and gallops. *J Exp Biol.* **207**, 1027–1042.
28. Cronin TW, Kinloch MR, Olsen GH. 2007 Head-bobbing behavior in walking whooping cranes (Grus americana) and sandhill cranes (Grus canadensis). *Journal of Ornithology* **148**, 563–569.
29. Necker R. 07 Head-bobbing of walking birds. *Journal of comparative physiology. A, Neuroethology, sensory, neural, and behavioral physiology* **193**, 1177–1183.
30. Dunbar DC, Macpherson JM, Simmons RW, Zarcades A. 2008 Stabilization and mobility of the head, neck and trunk in horses during overground locomotion: comparisons with humans and other primates. *J Exp Biol.* **211**, 3889–3907.
31. Xiang, Y.and Yakushin SB, Kunin M, Raphan T, Cohen B. 2008 Head stabilization by vestibulocollic reflexes during quadrupedal locomotion in monkey. *J Neurophysiol.* **100**, 763–780.
32. Paoletti P, Mahadevan L. 2012 Balancing on tightropes and slacklines. *Journal of the Royal Society, Interface* **9**, 2097–108.
33. Farkhatdinov I, Michalska H, Berthoz A, Hayward V. 2019 pp. 185–209. In *Review of Anthropomorphic Head Stabilisation and Verticality Estimation in Robots*, pp. 185–209. Cham: Springer International Publishing.
34. Kalman RE. 1960 A new approach to linear filtering and prediction problems 1. *Transactions of the ASME Journal of Basic Engineering* **82**, 35–45.
35. Dimiccoli M, Girard B, Berthoz A, Bennequin D. 2013 Striola magica. A functional explanation of otolith geometry. *Journal of computational neuroscience* **35**, 125–154.
36. Jaeger R, Haslwanter T. 2004 Otolith responses to dynamical stimuli: results of a numerical investigation. *Biological cybernetics* **90**, 165–75.
37. Takagi A, Sando I. 1988 Computer-Aided Three-Dimensional Reconstruction and Measurement of the Vestibular End-Organs. *Otolaryngol Head Neck Surg* **98**, 195–202.
38. De Vries H. 1951 The mechanics of the labyrinth otoliths. *Acta Oto-Laryngologica* **38**, 262–73.
39. Chaturvedi N, Sanyal A, McClamroch N. 2011 Rigid-body attitude control. *IEEE Control Systems* **31**, 30–51.
40. Diop S, Fliess M. 1991 Nonlinear observability, identifiability, and persistent trajectories. In *Proceedings of the 30th IEEE Conference on Decision and Control* pp. 714–719.

41. Hermann R, Krener A. 1977 Nonlinear controllability and observability. *IEEE Transactions on Automatic Control* **22**, 728–740.
42. Diop S. 2001 The algebraic theory of nonlinear observability revisited. In *Proceedings of the 40th IEEE Conference on. IEEE Decision and Control* pp. 2550–2555.
43. Sedoglavic A. 2001 A probabilistic algorithm to test local algebraic observability in polynomial time. In Mourrain B, editor, *Proceedings of the 2001 International Symposium on Symbolic and Algebraic Computation* pp. 309–316.
44. Fransson M, Gréen H. 2008 Comparison of two types of population pharmacokinetic model structures of paclitaxel. *European Journal of Pharmaceutical Sciences* **33**, 128–37.
45. Jiménez-Hornero JE, Santos-Dueñas IM, Garci A-Garci A I. 2008 Structural identifiability of a model for the acetic acid fermentation process. *Mathematical Biosciences* **216**, 154–62.
46. Liu YY, Slotine JJ, Barabási AL. 2013 Observability of complex systems. *Proceedings of the National Academy of Sciences of the United States of America* **110**, 2460–2465.
47. Golubev A, Krishchenko A, Tkachev S. 2002 Separation principle for a class of nonlinear systems. In *Proceedings of the 15th IFAC World Congress, 2002* vol. 15.
48. Luenberger DG. 1964 Observing the state of a linear system. *IEEE Trans. Mil. Electron.* **8**, 74–80.
49. Seidman SH, Telford L, Paige GD. 1998 Tilt perception during dynamic linear acceleration.. *Experimental brain research* **119**, 307–314.
50. Angelaki DE, Wei M, Merfeld DM. 2001 Vestibular discrimination of gravity and translational acceleration. *Annals of the New York Academy of Sciences* **942**, 114–127.
51. Glasauer S. 1992 Interaction of semi circular canals and otoliths in the processing structure of the subjective zenith. *Annals of the New York Academy of Sciences* **656**.
52. Merfeld DM, Young LR. 1993 A multidimensional model of the effect of gravity on the spatial orientation of the monkey. *Journal of vestibular research: equilibrium & orientation*.
53. Glasauer S, Merfeld DM. 1997 Modelling three-dimensional vestibular responses during complex motion stimulation. In Fetter M, Haslwanter T, H M, editors, *Three-dimensional kinematics of eye, head and limb movements* pp. 387–398. Amsterdam: Harwood Academic.
54. Merfeld DM, Zupan L, Peterka RJ. 1999 Humans use internal models to estimate gravity and linear acceleration. *Nature* **398**, 615–618.
55. Merfeld DM, Zupan LH. 2002 Neural processing of gravitoinertial cues in humans. III Modeling tilt and translation responses. *J Neurophysiol.* **87**, 819–833.
56. Merfeld DM, Zupan LH, Gifford CA. 2001 Neural Processing of Gravito-Inertial Cues in Humans. II. Influence of the Semicircular Canals During Eccentric Rotation. *J Neurophysiol.* **85**, 1648–1660.
57. Laurens J, Droulez J. 2007 Bayesian processing of vestibular information. *Biol Cybern.* **96**, 389–404.
58. Laurens J, Straumann D, Hess BJM. 2010 Processing of angular motion and gravity information through an internal model. *J Neurophysiol.* **104**, 1370–1381.
59. Laurens, J. SD, Hess BJ. 2011 Spinning versus Wobbling: How the Brain Solves a Geometry Problem. *The Journal of Neuroscience* **31**, 8093–8101.
60. Goldberg JM, Fernández C. 1975 Vestibular mechanisms. *Ann. rev. of physiology* **37**, 129–62.
61. Yoganandan N, Pintar FA, Zhang, J.and Baisden JL. 2009 Physical properties of the human head: mass, center of gravity and moment of inertia. *Journal of Biomechanics* **42**, 1177–92.
62. Menz HB, Lord SR, Fitzpatrick RC. 2003 Acceleration patterns of the head and pelvis when walking on level and irregular surfaces. *Gait & Posture* **18**, 35–46.
63. Farkhatdinov I, Hayward V, Berthoz A. 2011 On the benefits of head stabilization with a view to control balance and locomotion in humanoids. In *11th IEEE-RAS International Conference on Humanoid Robots 2011* pp. 147–152.
64. Benallegue M, Laumond JP, Berthoz A. 2013 Contribution of actuated head and trunk to passive walkers stabilization. In *IEEE Int. Conf. on Robotics and Automation* pp. 5638–5643.
65. Kryczka P, Falotico E, Hashimoto K, Lim H, Takanishi A, Laschi C, Dario P, Berthoz A. 2012 Implementation of a human model for head stabilization on a humanoid platform. In *2012 4th IEEE RAS & EMBS International Conference on Biomedical Robotics and Biomechatronics (BioRob)* pp. 675–680. IEEE.
66. Farkhatdinov I, Michalska H, Berthoz A, Hayward V. 2013 Modeling verticality estimation during locomotion. In *Romansy 19–Robot Design, Dynamics and Control* pp. 359–366. Springer.
67. Falotico E, Cauli N, Kryczka P, Hashimoto K, Berthoz A, Takanishi A, Dario P, Laschi C. 2017 Head stabilization in a humanoid robot: models and implementations. *Autonomous Robots* **41**, 349–365.

68. Farkhatdinov I, Roehri N, Burdet E. 2017 Anticipatory detection of turning in humans for intuitive control of robotic mobility assistance. *Bioinspiration & biomimetics* **12**, 055004.
69. Farkhatdinov I, Ebert J, van Oort G, Vlutters M, van Asseldonk E, Burdet E. 2019 Assisting Human Balance in Standing With a Robotic Exoskeleton. *IEEE Robotics and Automation Letters* **4**, 414–421.